Iraqi National Journal of Earth Science
www.earth.mosuljournals.com

Hydrogeochemical Evaluation of Groundwater In Sulaymaniyah-Sharazoor Basin, Kurdistan, NE Iraq

Halmat A. Saleh[1*], Diary A. Al-Manmi [2], Hadi Sanikhani [3]

[1]*Department of Geology, College of Science, University of Sulaimani, Sulaymaniyah, Iraq.*
[2]*Department of Petroleum and Energy Engineering, Technical College of Engineering, Sulaimani Polytechnic University, Sulaymaniyah, Iraq.*
[3]*Department of Water Sciences and Engineering, Faculty of Agriculture, University of Kurdistan, Sanandaj, Iran.*

Article information

Received: 29- -June -2023

Revised: 20- Aug -2023

Accepted: 04- Sep -2023

Available online: 01- Jan – 2024

Keywords:
Hydrogeochemistry
Modeling
NETPATHWin
Reaction transport
Kurdistan

Correspondence:
Name: Halmat Ali Saleh

Email: halmat.ali@univsul.edu.iq

ABSTRACT

Groundwater quality evaluation, the spatial distribution of quality parameters, and hydrogeochemical modeling are useful tools for decision-makers in water quality management. The present study has applied GIS techniques for groundwater spatial distribution and hydrogeochemical model using NETPATHWin software for groundwater evaluation for drinking purpose in the Sulaymaniyah-Sharazoor basin. Sampling from thirty-one wells and seven springs was done, and major cations, anions, and NO_3 were analyzed. The results show that all groundwater samples are suitable for different purposes according to Iraqi and World Health Organization standards and are characterized by low dissolved solid content. The northeastern and center of the basin are characterized relatively by higher contents of dissolved solids. Four flow paths were taken along the groundwater direction, and the output for the selected models revealed that the main hydrogeochemical reaction is dissolution-precipitation, and in some cases, there is cation exchange. Furthermore, the majority of water samples are undersaturated with concerning calcite, aragonite, dolomite, gypsum, anhydrite, and halite.

DOI: 10.33899/earth.2023.141301.1102,

التقييم الهيدروجيوكيميائي للمياه الجوفية لحوض سليمانية– شهرزور، كردستان، شمال شرق العراق

هه لمه ت علي صالح [1*]، ديار ي علي محمد امين [2] ، هادي سانيخاني [3]

[1] قسم علم الأرض ، كلية العلوم، جامعة السليمانية، السليمانية، العراق.

[2] قسم هندسة النفط و الطاقة، كلية الهندسة التقنية، جامعة السليمانية التقنية، السليمانية، العراق.

[3] قسم علوم المياه والهندسة، كلية الزراعة، جامعة كردستان، سنندج، ايران.

معلومات الارشفة

تاريخ الاستلام: 29– يونيو –2023

تاريخ المراجعة: 20– أغسطس –2023

تاريخ القبول: 04– سبتمبر –2023

تاريخ النشر الالكتروني: 01– ديسمبر –2024

الكلمات المفتاحية:

الهيدروجيوكيمياء

الانموذج NETPATHWin

نقل التفاعل

كوردستان

المراسلة:

الاسم: هه لمه ت علي صالح

Email :halmat.ali@univsul.edu.iq

الملخص

يعد تقييم نوعية المياه الجوفية، والتوزيع المكاني لمعايير النوعية، والنمذجة الهيدروجيوكيميائية أدوات مفيدة لصانعي القرار في إدارة نوعية المياه. في الدراسة الحالية تم تطبيق تقنيات نظم المعلومات الجغرافية للتوزيع المكاني للمياه الجوفية و نموذج هيدروجيوكيميائي باستخدام برنامج NETPATHWin لتقييم المياه الجوفية في حوض السليمانية – شهرزور. تم أخذ العينات من واحد وثلاثين بئراً وسبعة ينابيع، وتم تحليل الايونات الموجبة والسالبة الرئيسية وايون النترات. بينت النتائج أن جميع عينات المياه الجوفية مناسبة لأغراض مختلفة حسب المعايير العراقية ومعايير منظمة الصحة العالمية وتتميز بمحتوى واطئ من مواد الصلبة الذائبة. يتميز الجزء الشمالي الشرقي من الحوض ووسطه بمحتويات أعلى نسبيًا من المواد الصلبة الذائبة. تم أخذ أربع مسارات على طول اتجاه المياه الجوفية، وأظهرت نتائج النماذج المختارة أن التفاعل الهيدروجيوكيميائي الرئيسي هو الذوبان–الترسيب، وفي بعض الحالات، هناك تبادل الايوني. علاوة على ذلك، فإن غالبية عينات المياه غير مشبعة بالنسبة لمعادن كالسيت والأراغونايت والدولومايت والجبس والأنهيدرايت والهالايت.

DOI: 10.33899/earth.2023.141301.1102,

Introduction

The increase in population growth in urban and semi-urban areas and agricultural activities has led to an increase in the need for large quantities of water for drinking, agricultural, and industrial purposes especially in the Sulaymaniyah-Sharazoor basin (Al-Manmi, 2002, Al-Manmi et al., 2019). Due to this increase in such areas, there are many sources of pollution, as huge amounts of liquid and solid waste are thrown into surface and groundwater, leading to pollution. Water with certain physical and chemical characteristics may be suitable for agricultural uses, but not as a domestic water supply. Therefore, the study of water quality is of great importance to define the prime mode of use. The study of groundwater quality involves a description of the occurrence of the various constituents and the relationship of these constituents to the aquifer material (Al-Manmi, 2007).

Some researchers conducted studies on the groundwater quality, hydrogeochemical evaluation, geogenic sources of arsenic and fluoride in the Sulaymaniyah -Sharazoor basin (e.g. Abdullah et al., 2016; Abdullah et al., 2019; Mustafa et al., 2023).

Groundwater geochemistry is an overlapping science that deals with water chemistry in the subsurface environment, as the chemical composition of groundwater is the dual result of water entering the aquifer and interactions with rocks containing various minerals (Appelo, 1999). Groundwater also has a wide range of chemical composition (Drever, 1997; Appelo, 1999), and this wide range is the result of the difference in origin (marine, atmospheric, congenital, etc.) pollution, pressure, and temperature (Stuyfzand, 1999). Water hydrochemistry is of great importance in the process of evaluating groundwater resources because the quality of water is not less important than its quantity. In other words, the chemical, physical, and biological specifications are of great importance for determining the suitability of water for various uses. Drever (1997) identified some environmental factors that are closely related to water chemistry, such as the type of rocks, climate, relief, vegetation, and time.

Dissolution and precipitation of minerals, redox reactions, oxidation of organic matter, and ion exchange processes in aquifers can control the variation in the chemistry of the main elements of groundwater (Varsanyi et al., 1997; Merkel, et al., 2005; Ahmed and Clark, 2016; Al-Ghanimy et al., 2019; Hussein et al., 2021). In order to understand these factors and the effect of the groundwater flow path on these interactions, hydrogeochemical modeling is used by applying advanced softwares such as WATEQ4F developed by Ball et al. (1994), and NETPATHWin developed by Plummer et al. (1996).

The most essential capability that differentiates NETPATH (and NETPATH-WIN) from PHREEQC is in the treatment of radiocarbon dating of dissolved samples. This is where NETPATH excels over PHREEQC (Parkhurst and Appelo, 1999).

The application of well-known radiocarbon adjustment models to water samples is one of the capabilities of NETPATH (and NETPATH-WIN) that is not currently available in PHREEQC. The other capability is the solving of the Wigley et al. (1978) isotope evolution equations, which automatically calculate the relevant isotopic compositions of exsolving or precipitating phases and allow for the calculation of ^{14}C geochemical dilution and isotope fractionation adjustments in radiocarbon dating of dissolved carbon.

Hydrogeochemical modeling is defined as the optimal method through which it is possible to interpret or predict the chemical interactions of minerals, gases, and organic materials with aqueous solutions in real or hypothetical water-rock systems. Water-rock interactions are involved in the formation of basic ore deposits, crystallized and metamorphic rocks, transformational processes, and the decomposition of organic matter (Plummer, 1992; Parkhurst and Charlton, 2008). In modeling any chemical reaction, it is important to use the available information (Plummer, 1992) to find the dominant interaction, the extent to which the interaction reaches, and the conditions in which the reaction took place.

The process of modeling a chemical reaction requires extensive experience and can be simplified based on the following calculations: equilibrium speciation, mass balance, and reaction Path (Plummer et al., 1983; Plummer, 1992).

The facies distribution calculations (speciation calculations) determine the saturation state of the studied system with various minerals and specific gases based on the thermodynamic model and information about the water quality. Through these calculations, it is possible to predict whether the specified mineral will dissolve or precipitate under the given water conditions (Al-Mansoori, 2000; Al-Adili and Ali, 2005; Parkhurst and Charlton, 2008; Yang et al., 2018). As for the mass balance calculations, they determine the assumed mineral

quantities of the products and reactants that must dissolve or precipitate between the initial and final points in the system in order to determine the quality of the observed water.

In general, many interactions are considered important in the process of hydro-geochemical modeling, the most important of which are the formation of complexes or ion pairs in aqueous solutions (liquid phase), adsorption on solid surfaces (inter-phases), and precipitation or dissolution of solids (solid phase), redox reactions, hydration, alkaline and acid reactions, and isotopic processes (Domenico and Schwartz, 1998; Langmuir, 1997; Drever, 1997; Al-Shamari, 2017; Mahmmud et al., 2022). Knowing the distribution of free ions and ionic pairs is important in many studies, especially those related to groundwater contamination with heavy elements. The interactions that contribute to the formation of ionic complexes play an important role in highly saline groundwater, as many of these complexes facilitate the process of metal transfer. Toxic substances such as cadmium, chromium, etc. (Domenico and Schwartz, 1998; Plummer et al., 2004).

There are two types of modeling of water-rock interactions: forward modeling and inverse modeling. Forward modeling is a method in which a hypothetical reaction model is applied to certain initial conditions to predict the chemical composition of water and rocks as a function of the continuation of the reaction. This type of modeling can be used to predict the details of the reaction paths according to thermodynamic considerations between the initial and final points of the studied system (Plummer et al., 1983; Kumar et al., 2011; Parkhurst, and Appelo, 1999), provided that each path is defined by the mass transformations obtained from the inverse modeling.

In general, it can be said that the reverse modeling process is used to derive the chemical reactions in light of which the amount of change in the chemical composition of water along the flow path is determined. This can be done depending on the availability of chemical analyses for specific points along the flow path (Al-Mansoori, 2000; Al-Manmi, 2002; Khosravi et al., 2020). The main aims of this study are to evaluate groundwater quality for drinking purposes and predicting hydrochemical phases of reaction transport modeling depending on chemical parameters.

Study area

Sulaymaniyah-Sharazoor basin is located in the north-east of Iraq between latitudes N 35º 5′ 00″ and N 35º 45′ 00″ and the longitudes E 45º 10′ 00″ and E 46º 15′ 00″ (Fig. 1), with an area of 2503 km^2. It is located within the Tanjero Sub-basin, which has an area of 3034 km^2 (Polsevice, 1980; Al-Tamimi, 2007), and is one of the secondary basins of the Diyala Basin (Fig. 1). The area consists of four sub-basins: Sulaimani sub-basin, Arbat-Zarain sub-basin, Said Sadiq sub-basin, and Halabja-Khurmal sub-basin (Ali, 2007).

The topography's elevation ranges from 494 to 1533 meters above sea level. The study area encompasses a total of six different subdistricts in addition to Sulaymaniyah and Halabja Municipal Centre. These subdistricts are referred to as Arbat, Said Sadiq, Warmawa, Khormal, Byara, and Sirwan.

The climate of the study area is characterized as hot and dry in the summer and cold and wet in the winter. The region is under the influence of the Mediterranean front, and as a result of the collision of the cold European air mass and the hot air mass coming from South Africa, depressions occur in the winter season leading to a decrease in temperatures and snowfall.

According to the data obtained from Sulaymaniyah Meteorological Station for the period of 2000–2022, the study area is characterized by seasonal monthly rates of rainfall ranging between 30.1 and 120.1 mm/month, and the maximum seasonal annual average rainfall occurred in 2018–2019 with 1317.2 mm and the minimum seasonal annual average rainfall occurred in 2020–2021 with 410.5 mm.

Stratigraphy of the basin

The importance of studying the geological formations that carry groundwater comes from their impact on the properties of the water that passes through them and their reflection on the variation in the chemical characteristics of water in different aquifers. The study area covers many geological formations consisting of sedimentary rocks, represented by a number of sedimentary cycles. The oldest exposed rocks are the Early Cretaceous (Valanjian) rocks represented by the Avraman Formation (Triassic), and the most recent formations represented by the Sinjar Formation (Early Eocene) (Fig. 2). According to (Bellen et al., 1959; Buday, 1980; Jassim and Goff, 2006), the geological setting is described as follows:

The Avraman Formation consists of grey, thick-bedded, pure limestone and contains many fossils, with a total thickness of 3000 meters. Sargelu and Barsarin formations (Middle and Upper Jurassic). Sargalu consists of well-bedded and well crystallized, black bituminous limestone and dolomitic limestone and occasionally contains shells of Posidonia. The lower part is massive and thick forming a cliff. Barsarine exists as thin bedded, stromatolitic limestone. The Qulqula Formation (Albian-Bareemian) is composed of very thick packages of chert, marls, siliceous shale, and limestone beds. The Valanginian-Turonian age is represented by the Balambo Formation; the lower part consists of thin layers of ammonite-infused limestone with intercalation of green marl rocks. Its thickness is 59 m in the typical section, while the upper part consists of thin successions of limestone filled with Radiolaria fossils; its thickness is 503 m.

The Kometan Formation (Turonian) consists of thin, light-colored layers of limestone containing partly Oligostegina in its type locality section. The Shiranish Formation (Campanian-Maastrichtian) has a thickness of 220 m at its lower part. It consists of a succession of gray-colored marl limestone, highly jointed, and contains pyrite nodules and iron oxides.

The Tanjero Formation (Maastrichtian) generally consists of sandstone and marl of olive-gray color and conglomerate.

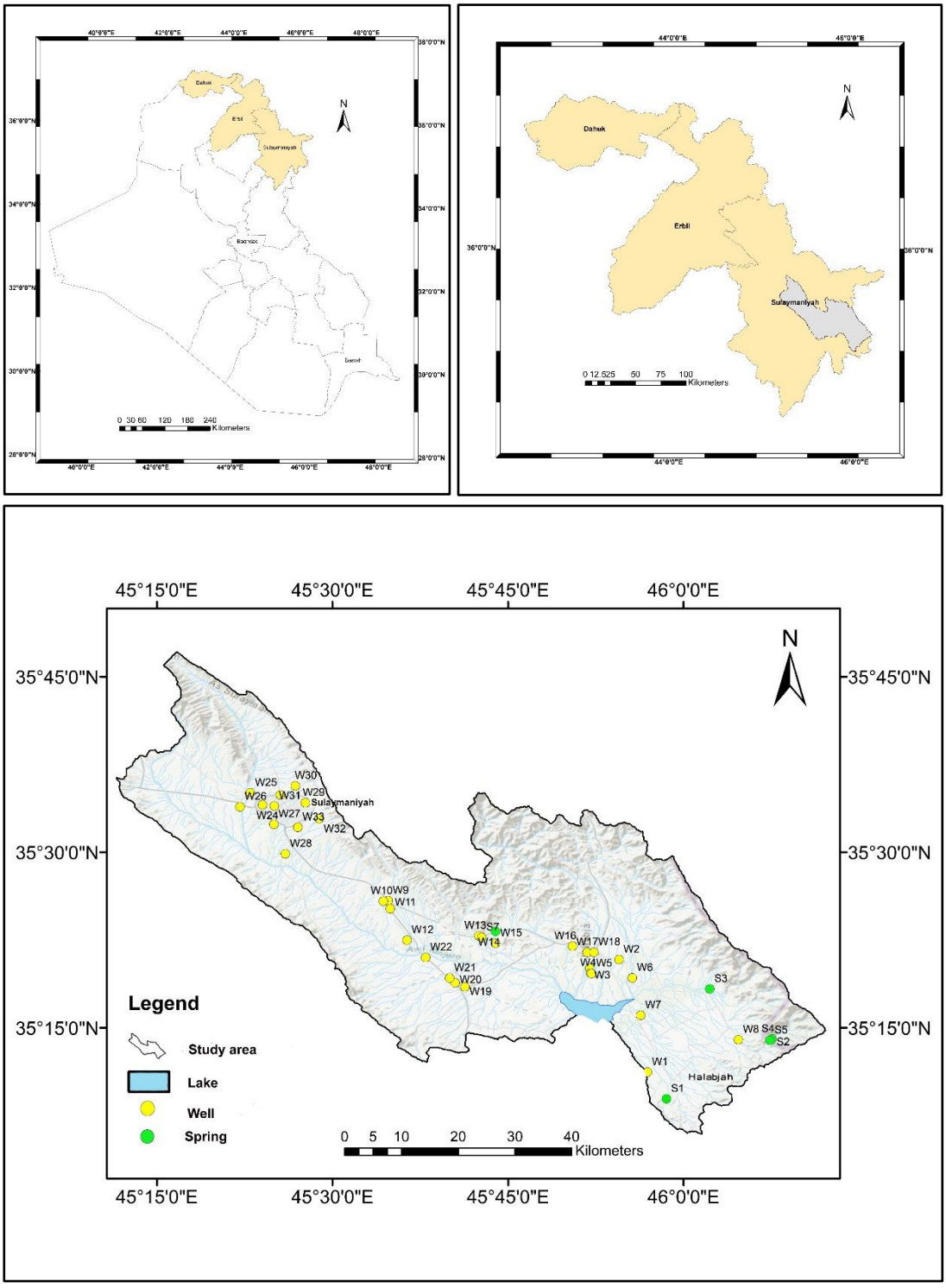

Fig. 1. Location map of the study area

The Kolosh, Sinjar, Gercus, and Pila Spi formations are examples of the tertiary sequence. Kolosh Formation (Paleocene) contains more shale and marl and less sandstone, while Sinjar Formation (Early Eocene) is thick-bedded fossiliferous limestone. The Gercus Formation (Middle Eocene) is made up of clastic rocks such as claystone, sandstone, marl, and calcareous shale, as well as conglomerate. The last formation that belongs to the Late Eocene is the Pila Spi Formation, which is composed of white, chalky, and dolomitic limestone.

Hydrogeologically, the Cretaceous carbonate rocks cover most parts of the study area, which represent the main water bearing formations, and these rocks are characterized by

containing two types of porosity (primary and secondary). There is a good amount of water in these formations, and the structural situation has an important role in the hydrogeology of the area.

The Karstic-Fissured Aquifer (KFA) is represented by the Balambo, Kometan, and Qamchuqa formations (mostly marly limestone, dolomitic limestone, limestone, and dolomite) (Stevanovic and Markovic, 2004b; Ali, 2007; Al-Manmi and Saleh, 2019). The aquifer is largely distinguished by its high transmissivity; in addition, it is extremely fissured and contains a large number of high-density fractures. In comparison to karstic aquifers, it has a shorter extent of fractures than other types of aquifers. The Cretaceous Karstic-Fissured Aquifer (CKFA) is the most major unit. This unit has extremely porous, solution channels, cavities, and tension fractures. Additionally, the bedding plane is highly jointed in this unit. The massiveness of the formation makes it difficult to see the set of joints, but if the thickness of the beds is reduced to one meter, at least two sets of joints can be distinguished from each other. The aquiclude is denoted by the Shiranish Formation. The effect of weathering and the degree to which the land has been deformed both cause variations in the thickness and compaction of aquiclude beds. Because of the unique properties, it possesses storing and releasing groundwater. The Tanjero Formation plays a dual role in the region of interest, performing the functions of both an aquitard and an aquiclude. Shale and marl make up the Tanjaro Formation, which enables geologists to classify it as an aquitard due to its geological make-up.

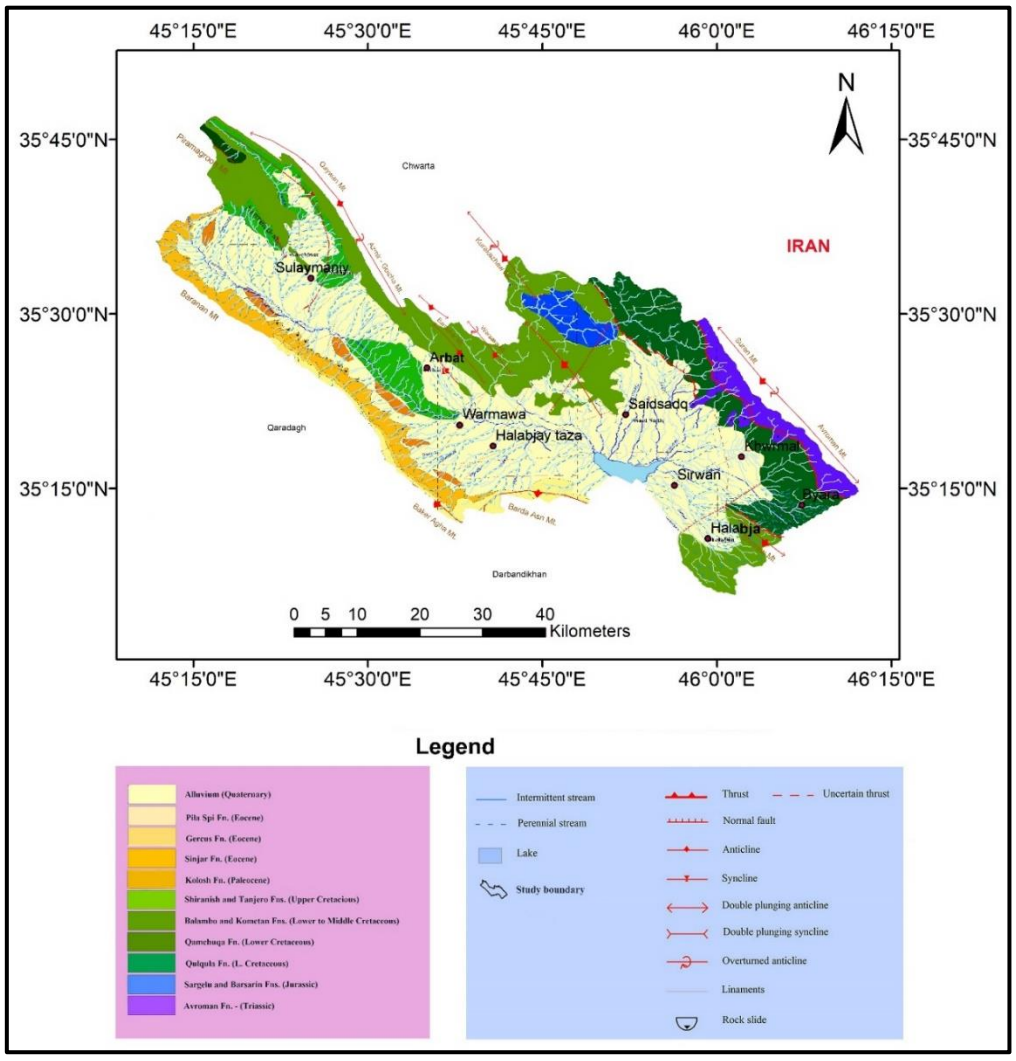

Fig. 2. Geological map of the study area

Materials and Methods

Water sampling

Water samples from 27 deep wells, 6 shallow wells, and 7 springs were collected on November 10, 2021(Fig. 3). The samples were collected in 500-ml polyethylene bottles after being washed well with distilled water and dilute hydrochloric acid before being taken to the field. During transport from the investigation area to the local laboratory, all samples were stored in a cooling box. In the laboratory, samples were stored in the fridge at approximately 8°C until analyses were carried out. The pH, electrical conductivity, redox potential, and temperature were measured directly in the field with multi-parameter devices (WorkCyberScan PC 300 and pH 300). The device is calibrated with distilled water, and calibration and checks of the functionality of the instruments were carried out before the field day.

The ions (Ca^{2+}, Mg^{2+}, HCO_3^-, and Cl^-) are measured titrimetrically, and Na^+ and K^+ are measured by flame photometer, while SO_4^{2-} is measured colorimetrically according to American Public Health Association (APHA, 2017) guidelines. Finally, the NO_3^- ion is analyzed using a spectrophotometer. The analyses of major ions are carried out at the Sulaymaniyah Health Protection Directorate, Iraq. A charge balance was calculated for each analysis to evaluate analytical error and to determine if all the major ions are accounted for in the analysis, and most of them are below 5%, considered acceptable for most water analyses.

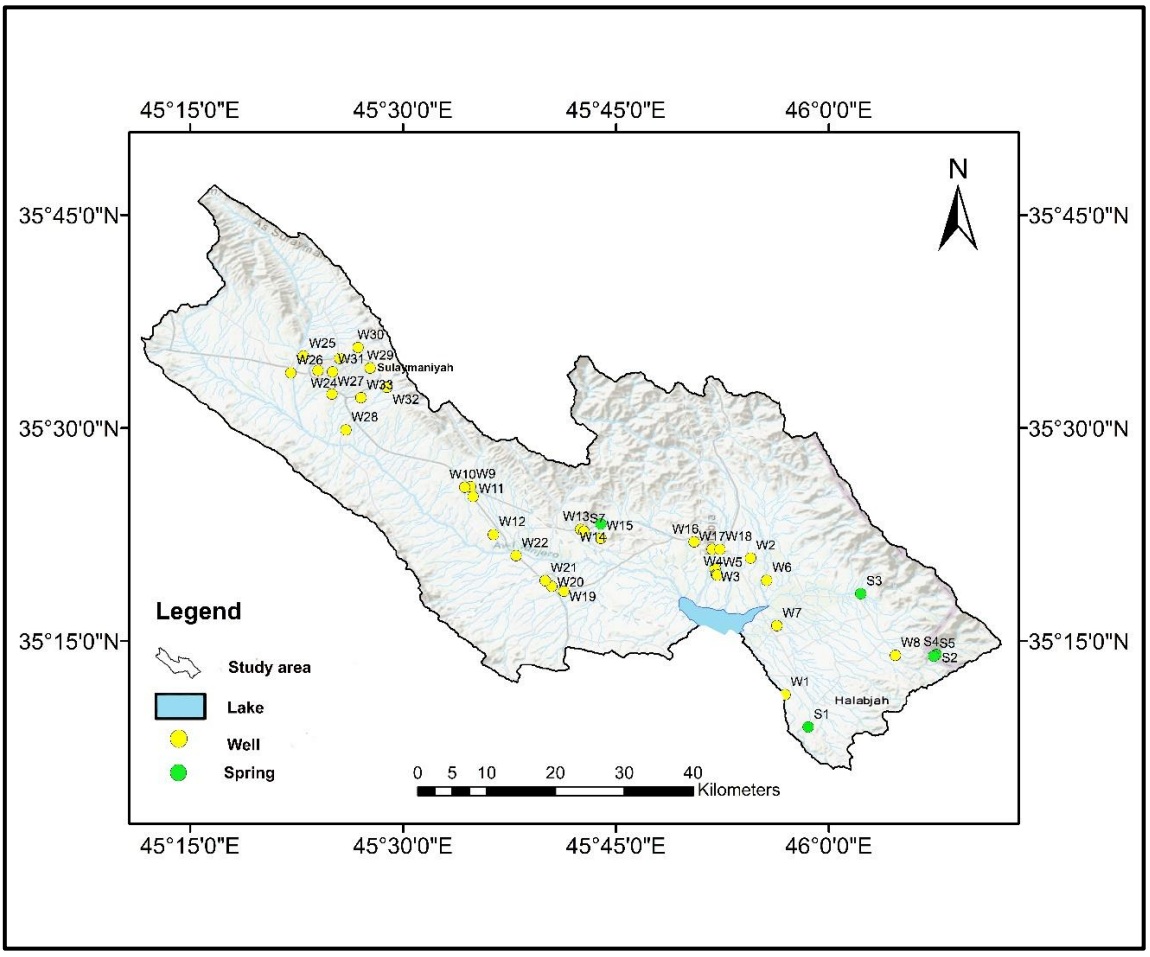

Fig. 3. Location of the water samples

Calculations of Saturation Indices

Saturation indices express the extent of chemical equilibrium between water and mineral phases in the matrix of the aquifers and could be regarded as a measure of dissolution and/or precipitation processes relating to the water rock interaction (Drever, 1997; Domenico, and Schwartz, 1998). The calculation of water saturation degree concerning solid mineral phases can be reached as in the following equation (Drever, 1997, Masoud et al., 2022):

$$SI_x = \log \frac{IAP\ (T)}{Ksp\ (T)} \quad \ldots\ldots\ldots\ldots (1)$$

Where:

SI_x: is the saturation index of mineral x,

IAP (T): is the ion activity products at specified temperature (^oC),

Ksp: is the equilibrium solubility product constant of mineral x.

The resulting values indicate whether the solution is undersaturated (-SIx), supersaturated (+SIx), or at equilibrium (SIx = 0) with respect to the mineral in question.

Theoretical CO_2 Partial Pressures calculation

The P_{CO2} is considered the most important factor controlling the precipitation and dissolution of carbonate minerals. Groundwater contains more (CO_2) than surface water due to the decomposition of organic matter in the topsoil layer.

P_{CO2} can be calculated by equation (2) below (Langmuir, 1997):

Where:

K_{CO2} is the equilibrium (Henry's law) constant for CO_2

K_1 is the first dissociation constant of H_2CO_3

Using the computer software *WATEQ4F*, saturation indices, ionic strength, and log P_{CO2} for different mineral phases are calculated.

Results

Groundwater chemistry

Table (1) summarizes the results of hydrochemical analysis, and the details are presented in the appendices (1 and 2). The groundwater of the basin is colorless and odorless, slightly alkaline, moderate hard to very hard, and is characterized by a low content of total dissolved salts, with an average of 232 mg/l for the wells and 276 mg/l for the springs.

The calcium ion predominates over the cations, while the bicarbonate ion prevails over the anions. The center and the east part of the basin are characterized by relatively higher concentrations of TDS than the others (Fig. 4 a, b, and c).

The water samples of the study area are suitable for drinking according to the WHO (2022) standard for the main ions, except for Garawi Khwrmal spring, which had a TDS concentration of 1209.6 mg/l.

When the water samples are projected on the Durov diagram, they are in the area of Ca-HCO_3 type, except for Garawi Khwrmal spring, which is Ca-SO_4 type (Fig. 5).

Table 1: The hydrochemical parameter range and mean values for water samples

Parameters	Wells		Springs	
	Range	Mean	Range	Mean
Ca^{2+} (mg/l)	41 - 103	54	40 - 215	65
Mg^{2+} (mg/l)	6.8 - 27	12	10 - 95	15
Na^{+} (mg/l)	5.6 - 33	9.8	6.9 - 52	8.5
K^{+} (mg/l)	0 - 2.7	0.3	0.1 – 8.4	0.4
SO_4^{2-} (mg/l)	6.7 - 93	36	21 - 486	28
Cl^{-} (mg/l)	7 - 44	15	6 - 33	11
HCO_3^{-} (mg/l)	170 - 268	195	178 - 375	213
NO_3^{-} (mg/l)	1 - 68	24	7 - 18	10
T.H. (mg/l)	132 - 368	192.4	148 - 928	209.1
TDS (mg/l)	121.6 - 480	231.7	144.6-1209.6	276.5
EC µS/cm	190 - 750	362	226 - 1890	432
pH	6.92 - 8.4	7.26	6.5 – 8.54	7.25
Eh (mv)	-92.4-(-12.7)	-34.2	-95-8.8	-31
T °C	13.1 – 21.5	18.8	13.4 - 29	15.1

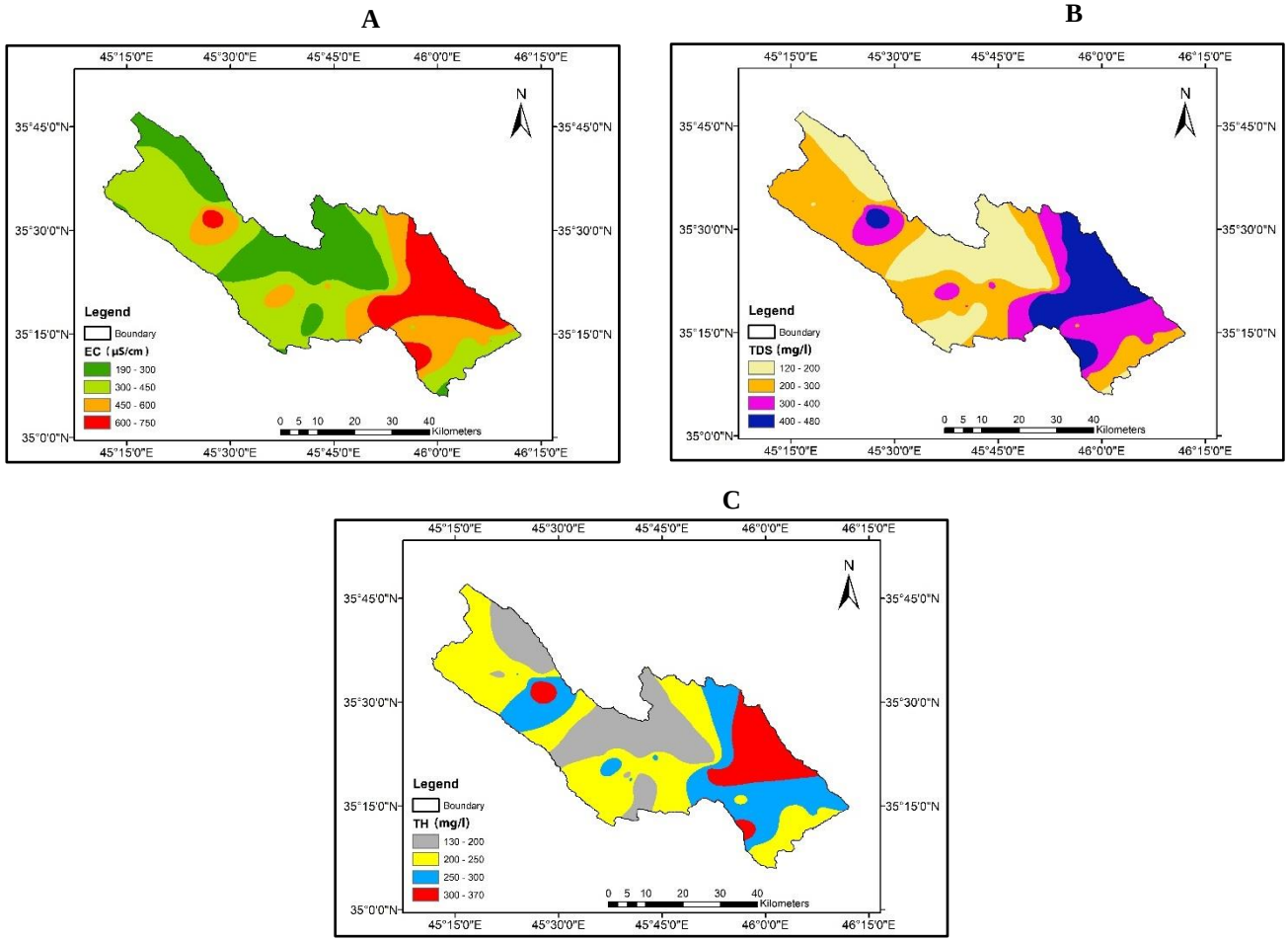

Fig. 4. Spatial distribution of EC (A), TDS (B), and TH (C) of the study area

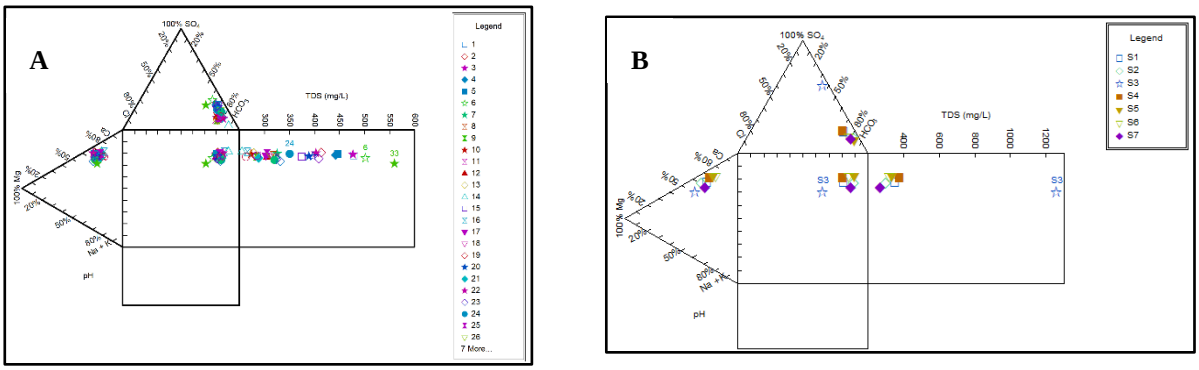

Fig.5. Durov diagram for (A) wells and (B) spring

Saturation Indices

Using the computer software WATEQ4F, saturation indices, ionic strength, and log PCO2 for different mineral phases are calculated, and the results of equilibrium speciation calculations for the study area are tabulated in Table (2).

According to the SI results of the groundwater in the study area, all water samples are undersaturated with halite, anhydrite, dolomite, aragonite, and gypsum minerals, except for some samples that are oversaturated with dolomite and aragonite, which means that the GW could dissolve more of these minerals. However, 30% of the water samples are oversaturated with calcite indicating the possibility of water precipitating these mineral species. The semi-arid climate in the study area may have led to the precipitation of dolomite, calcite, and aragonite due to low rainfall and high evaporation. Calcium, sodium, sulfate, and chloride components are not limited by the mineral equilibrium with anhydrite, gypsum, and halite (El Alfy et al., 2019; Al-Mashreki et al., 2023).

Table 2: Ionic strength, Log PCO_2, and minerals saturation Indices for wells and springs

Parameters and mineral phases	Ionic strength	Log P_{CO2}	SI Calcite	SI Aragonite	SI Dolomite	SI Gypsum	SI Anhydrite	SI Halite
W1	0.01114	-2.482	0.581	0.431	0.79	-1.651	-1.897	-8.285
W2	0.0091	-2.5	0.424	0.271	0.419	-1.897	-2.149	-8.415
W3	0.0107	-1.756	-0.108	-0.256	-0.6	-1.629	-1.869	-8.261
W4	0.0098	-1.995	-0.039	-0.191	-0.542	-1.695	-1.945	-8.236
W5	0.00998	-2.114	0.076	-0.076	-0.243	-1.685	-1.936	-8.474
W6	0.01148	-1.936	-0.017	-0.168	-0.448	-1.544	-1.793	-7.982
W7	0.00679	-2.308	0.089	-0.06	-0.295	-2.196	-2.439	-8.318
W8	0.00655	-3.183	0.901	0.753	1.385	-2.255	-2.494	-8.26
W9	0.00575	-1.877	-0.489	-0.636	-1.347	-2.445	-2.682	-8.347
W10	0.00525	-2.285	-0.112	-0.26	-0.644	-2.429	-2.666	-8.518
W11	0.00585	-1.977	-0.366	-0.513	-1.133	-2.423	-2.658	-8.297
W12	0.00655	-1.864	-0.427	-0.575	-1.285	-2.244	-2.482	-8.249
W13	0.00539	-1.779	-0.584	-0.732	-1.593	-2.439	-2.678	-8.456
W14	0.00475	-2.067	-0.308	-0.456	-1.085	-2.884	-3.123	-8.842
W15	0.00838	-1.631	-0.438	-0.585	-1.247	-1.903	-2.139	-8.278
W16	0.00525	-2.485	0.107	-0.039	-0.292	-2.285	-2.518	-8.88
W17	0.00614	-1.761	-0.552	-0.699	-1.509	-2.113	-2.349	-8.525
W18	0.00656	-1.969	-0.367	-0.516	-1.092	-1.965	-2.206	-8.633
W19	0.00563	-1.892	-0.516	-0.664	-1.496	-2.192	-2.432	-8.528
W20	0.00892	-1.702	-0.341	-0.488	-1.021	-1.852	-2.087	-8.368
W21	0.00563	-1.867	-0.48	-0.628	-1.379	-2.365	-2.606	-8.412
W22	0.00851	-2.144	0.225	0.077	0.15	-2.114	-2.355	-8.511
W23	0.0068	-2.356	0.078	-0.07	-0.153	-2.107	-2.347	-8.336
W24	0.0076	-1.96	-0.2	-0.349	-0.842	-1.939	-2.179	-8.347
W25	0.00637	-1.768	-0.496	-0.644	-1.441	-2.276	-2.517	-8.381

Parameters and mineral phases	Ionic strength	Log P_{CO2}	SI Calcite	SI Aragonite	SI Dolomite	SI Gypsum	SI Anhydrite	SI Halite
W26	0.00657	-1.739	-0.589	-0.738	-1.569	-2.063	-2.306	-8.63
W27	0.00691	-2.132	-0.13	-0.277	-0.536	-2.111	-2.348	-8.477
W28	0.00895	-2.207	0.153	0.005	-0.047	-1.819	-2.06	-8.334
W29	0.00584	-1.98	-0.372	-0.52	-1.143	-2.315	-2.554	-8.486
W30	0.005	-2.142	-0.319	-0.467	-1.148	-2.356	-2.597	-8.464
W31	0.00694	-1.993	-0.243	-0.391	-0.723	-2.072	-2.309	-8.401
W32	0.00909	-2.435	0.354	0.205	0.373	-1.801	-2.045	-8.178
W33	0.01271	-2.749	0.913	0.764	1.514	-1.574	-1.815	-7.413
S1	0.00736	-2.067	-0.124	-0.273	-0.59	-2.006	-2.249	-8.38
S2	0.00626	-3.34	0.894	0.741	1.481	-2.275	-2.527	-8.92
S3	0.03356	-0.953	-0.216	-0.357	-0.407	-0.78	-0.983	-7.407
S4	0.00827	-1.985	-0.165	-0.317	-0.785	-1.891	-2.141	-8.39
S5	0.00732	-1.976	-0.165	-0.316	-0.863	-2.197	-2.446	-8.793
S6	0.00669	-2.311	0.022	-0.13	-0.587	-2.114	-2.366	-8.568
S7	0.00526	-1.798	-0.676	-0.825	-1.633	-2.415	-2.658	-8.602
Min.	0.00475	-3.34	-0.676	-0.825	-1.633	-2.884	-3.123	-8.92
Max.	0.03356	-0.953	0.913	0.764	1.514	-0.78	-0.983	-7.407
Mean	0.00804	-2.087	-0.101	-0.249	-0.590	-2.058	-2.299	-8.390
		PCO2 (Bar)			Ionic Strength (mol/Kg)			

Corrosivity and Scale Formation

Corrosion is the result of a complicated chain of chemical reactions that took place between water and the surfaces of metals, as well as the materials that are used to store or transport water. A reaction involving oxidation and reduction, corrosion is the process by which refined or processed metals are converted back to their more stable ore condition. The potential presence of toxic metals such as lead and copper, the deterioration and damage to household plumbing, and aesthetic problems such as stained laundry, a bitter taste, and greenish-blue stains around basins and drains are the primary concerns regarding the corrosion potential of water. Other concerns include the potential presence of toxic metals such as lead and copper. In soft water, corrosion takes place because there are not enough dissolved cations like calcium and magnesium; on the other hand, in hard water, a precipitate or coating of calcium or magnesium carbonate builds up on the internal wall of pipes. This makes soft water more susceptible to damage from corrosion. The fact that this coating functions as a barrier means that it can prevent the pipe from corroding, but it also has the potential to clog the pipe. The conductivity of water is increased and corrosion is encouraged when it contains large concentrations of ions such as sodium, chloride, or other ions (Melidis et al., 2007; Wang, and Luo, 2001; Al-Qurnawi et al., 2022). The use of saturation indices as a measure of the corrosivity of water or the production of scale was common. Table (3) gives a typical range of SI of calcite that may be found in drinking water, together with a description of the composition of the water and basic suggestions about treatment (W.U., C.E.G, G.S.E. Dept., 2002).

According to the saturation indices of minerals in the investigated groundwater samples (Table 4) as indicators of water corrosivity or scale formation, the following could be deduced:

-The majority of groundwater samples (70%) shows mild corrosion. Treatment should be considered.

-Wells, W1, W2, W22, W31, and spring S6 have some faint coating; therefore, treatment is typically not needed.

Table 3: Classification of water corrosion potential based on the calcite saturation indices values and recommended treatments (Adopted from Gomaa et al., 2014)

Saturation indices (SI)	Description	General recommendations
-5	Severe corrosion	Treatment recommended
-4	Moderate corrosion	Treatment recommended
-3	Moderate corrosion	Treatment recommended
-2	Moderate corrosion	Treatment should be considered
-1	Mild corrosion	Treatment should be considered
-0.5	Mild corrosion	Treatment should be considered
0	Balanced	Treatment typically not needed
0.5	Some faint coating	Treatment typically not needed
1	Mild scale forming	Some aesthetic problems
2	Mild scale forming	Some aesthetic problems
3	Moderate scale forming	Treatment should be considered
4	Severe scale forming	Treatment probably required
5	Severe scale forming	Treatment required

Table 4: Type of groundwater samples in the study area based corrosivity index

Sample No.	SI	Corrosivity	Sample No.	SI	Corrosivity
W1	0.581	Some faint coating	W22	0.225	Some faint coating
W2	0.424	Some faint coating	W23	0.078	Balanced
W3	-0.108	Mild corrosion	W24	-0.2	Mild corrosion
W4	-0.039	Mild corrosion	W25	-0.496	Mild corrosion
W5	0.076	Balanced	W26	-0.589	Mild corrosion
W6	-0.017	Mild corrosion	W27	-0.13	Mild corrosion
W7	0.089	Balanced	W28	0.153	Balanced
W8	0.901	Mild scale forming	W29	-0.372	Mild corrosion
W9	-0.489	Mild corrosion	W30	-0.319	Mild corrosion
W10	-0.112	Mild corrosion	W31	-0.243	Mild corrosion
W11	-0.366	Mild corrosion	W31	0.354	Some faint coating
W12	-0.427	Mild corrosion	W32	-0.496	Mild corrosion
W13	-0.584	Mild corrosion	W33	0.913	Mild scale forming
W14	-0.308	Mild corrosion	S1	-0.124	Mild corrosion
W15	-0.438	Mild corrosion	S2	0.894	Mild scale forming
W16	0.107	Balanced	S3	-0.216	Mild corrosion
W17	-0.552	Mild corrosion	S4	-0.165	Mild corrosion
W18	-0.367	Mild corrosion	S5	-0.165	Mild corrosion
W19	-0.516	Mild corrosion	S6	0.022	Some faint coating
W20	-0.341	Mild corrosion	S7	-0.676	Mild corrosion
W21	-0.48	Mild corrosion			

Reaction paths

For the purpose of studying the geochemical evolution of the groundwater system along the groundwater flow paths and quantifying the mass transformation of the selected mineral phases depending on the dominant chemical reactions, four groundwater paths were chosen (Fig. 6). Wells located in the recharge areas are used as primary wells, and wells located in the basin center and discharge areas are used as final wells. The interactive NETPATH-WIN computer program is used for inverse geochemical modeling (El-Kadi et al., 2011, Eissa et al., 2018; El Alfy, 2013; Eissa et al., 2014; Aghazadeh et al., 2017).

Below is an explanation and discussion of the selected paths:

1. Flow path 1

Wells (16, 3) are considered the initial and final wells for this path (Fig. 6); among the 36 checked models, only two are considered. Table (5) shows the amounts of mass transfer for the selected mineral phases, measured in mmol/kg H_2O. It is noted that calcite, dolomite, gypsum, and NaCl are dissolved and there is Ca-Na exchange in model 1, while in model 2, calcite,

dolomite, and gypsum are dissolved and there is Ca-Na exchange. Furthermore, the results show that CO_2 gas is released in both models. When comparing these results with the results of WATEQ4F, we conclude that during the flow path there is an increase in the solubility of calcite, gypsum, NaCl, and dolomite, which leads to an increase in the concentration of calcium, magnesium, and sulfates. We notice that well 3 has high values of these ions, and this is consistent with the values of (Log P_{CO_2}) because the values of this variable are high in the well 6, as the higher the value of Log P_{CO_2}, the more carbonate minerals will dissolve.

Table 5: Mass Transfer Model in (mmol / Kg H_2O) for selected mineral phases for path-1

Model 1(36 models checked)		
Mineral phases	**Mass transfer (mmol/Kg H_2O)**	**Process**
Calcite	0.62722	Dissolution
Dolomite	0.09023	Dissolution
Gypsum	0	Dissolution
NaCl	0.04027	Dissolution
Ca-Na Exchange	0.07650	Ca-Na Exchange
CO_2 gas	-0.05231	Released
Model 2		
Calcite	0.62722	Dissolution
Dolomite	0.09023	Dissolution
NaCl	0.04027	Dissolution
Ca-Na Exchange	0.07650	Ca-Na Exchange
CO_2 gas	-0.05231	Released

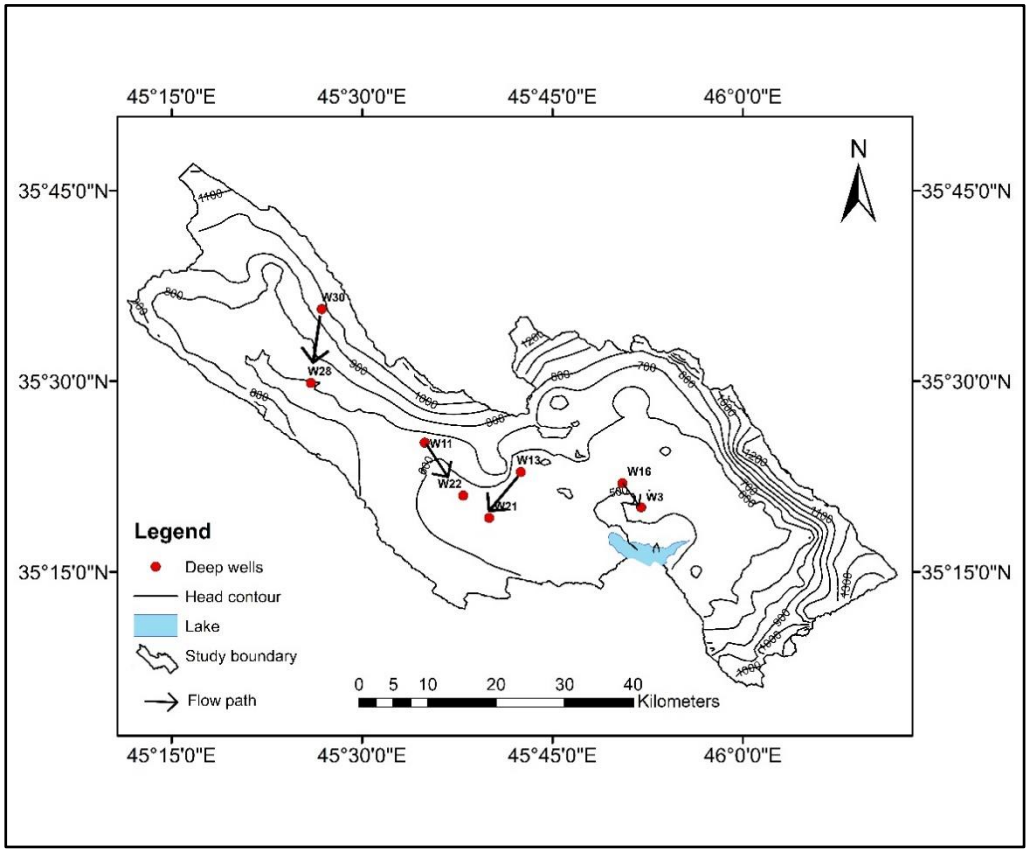

Fig.6. Selected wells and model paths for reaction transport modeling in the study area

2. Flow path 2

Wells (13, 21) are considered the initial and final wells for this path (Fig. 6); among the 36 checked models, only three are considered. Table (6) shows the amounts of mass transfer for the selected mineral phases, measured in mmol/kg H_2O. It is noted that calcite, dolomite, and NaCl are precipitated and there is Ca-Na exchange in model 1, 2, and 3 while in model 2, gypsum is dissolved. Furthermore, the results show that CO_2 gas is released in models 1 and 3. When comparing these results with the results of WATEQ4F, we conclude that during the flow path there is a slight decrease in the solubility of calcite, NaCl, and dolomite. Among the three models, models 1 and 3 are better fits than model 2.

Table 6: Mass Transfer Model in (mmol / Kg H_2O) for selected mineral phases for path-2

Model 1 (36 models checked)		
Mineral phases	**Mass transfer (mmol/Kg H_2O)**	**Process**
Calcite	-0.21995	Precipitation
Dolomite	-0.15914	Precipitation
NaCl	-0.28173	Precipitation
Ca-Na Exchange	0.13356	Ca-Na Exchange
CO_2 gas	-0.80581	Released
Model 2		
Calcite	-0.95852	Precipitation
Dolomite	-0.15914	Precipitation
Gypsum	0.73857	Dissolution
NaCl	-0.28173	Precipitation
Ca-Na Exchange	0.13356	Ca-Na Exchange
Model 3		
Calcite	-0.21995	Precipitation
Dolomite	-0.15914	Precipitation
NaCl	-0.28173	Precipitation
Ca-Na Exchange	0.13356	Ca-Na Exchange
CO_2 gas	-0.73857	Released

3. Flow path 3

Wells (11, 22) are considered the initial and final wells for this path (Fig. 6); among the 36 checked models, only three are considered. Table (7) shows the amounts of mass transfer for the selected mineral phases, measured in mmol/kg H_2O. It is noted that calcite, dolomite, gypsum, and NaCl are dissolved and there is Ca-Na exchange in all models, but in model 2, calcite is precipitated. Furthermore, the results show that CO_2 gas is released only in model 3. When comparing these results with the results of WATEQ4F, we conclude that during the flow path there is an increase in the solubility of calcite, gypsum, NaCl, and dolomite, which leads to an increase in the concentration of calcium, magnesium, and sulfates. We notice that the well 22 has high values of these ions, and this is consistent with the values of (Log P_{CO_2}) because the values of this variable are high in the well 22, as the higher the value of Log P_{CO_2}, the more carbonate minerals will dissolve. Among the three models, model 3 is a better fit than models 1 and 2.

Table 7: Mass Transfer Model in (mmol / Kg H_2O) for selected mineral phases for path-3

Model 1 (36 models checked)		
Mineral phases	**Mass transfer (mmol/Kg H_2O)**	**Process**
Calcite	9.87556	Dissolution
Dolomite	12.99982	Dissolution
Gypsum	4.96067	Dissolution
NaCl	6.40563	Dissolution
Ca-Na Exchange	-0.95587	Ca-Na Exchange
Model 2		
Calcite	-70.86518	Precipitation
Dolomite	12.99982	Dissolution
Gypsum	85.70142	Dissolution
NaCl	6.40563	Dissolution
Ca-Na Exchange	-0.95587	Ca-Na Exchange

	Model 3	
Calcite	9.87556	Dissolution
Dolomite	12.99982	Dissolution
Gypsum	4.96067	Dissolution
NaCl	6.40563	Dissolution
Ca-Na Exchange	-0.95587	Ca-Na Exchange
CO_2 gas	40.37037	Released

4. Flow path 4

Wells (30, 28) are considered the initial and final wells for this path (Fig. 6); among the 28 checked models, only two are considered. Table (8) shows the amounts of mass transfer for the selected mineral phases, measured in mmol/kg H_2O. It is noted that dolomite and gypsum are dissolved and there is Ca-Na exchange in all models, but calcite is precipitated in the two models. Furthermore, the results show that CO_2 gas is released only in model 2. When comparing these results with the results of WATEQ4F, we conclude that during the flow path there is an increase in the solubility of gypsum, NaCl, and dolomite, and the water in the well 28 is saturated with calcite. Among the three models, model 2 is a better fit than others.

Table 8: Mass Transfer Model in (mmol / Kg H_2O) for selected mineral phases for path-4

	Model 1 (28 models checked)	
Mineral phases	**Mass transfer (mmol/Kg H_2O)**	**Process**
Calcite	-0.33785	Precipitation
Dolomite	0.31532	Dissolution
Gypsum	0.48253	Dissolution
Ca-Na Exchange	0.00905	Ca-Na Exchange
	Model 2	
Calcite	-0.17057	Precipitation
Dolomite	0.31532	Dissolution
Gypsum	0.31525	Dissolution
Ca-Na Exchange	0.00905	Ca-Na Exchange
CO_2 gas	0.08364	Released

Conclusions

Groundwater quality evaluation and hydrogeochemical modeling for groundwater flow paths are crucial issues for allocating suitable water sources and predicting the hydrogeochemical processes and reactions that took place in the groundwater environment.

The groundwater chemistry of the study area is characterized by a low content of dissolved solids and Ca-HCO_3 as the predominant type. The lithology of the geological formations has a greater impact on the type of groundwater and the ions concentrations. The applied WATEQ4F and NETPATH$_{Win}$ models revealed that the majority of water samples are undersaturated for calcite, aragonite, dolomite, gypsum, anhydrite, and halite. The groundwater in the study area is controlled by dissolution and precipitation reactions. Furthermore, the solubility of some mineral phases such as calcite, gypsum, NaCl, and dolomite is increasing along the selected flow paths. Besides Ca-Na exchange taking place in some paths and CO_2 being released within the groundwater system.

Acknowledgements

Sincere thanks to the Sulaymaniyah Groundwater Directorate Department for providing water wells archive data.

Conflict of Interest

The authors declare that there is no conflict of interest.

References

Abdullah, T.O., Ali, S.S. and Al-Ansari, N.A. 2016. Groundwater assessment of Halabja Saidsadiq Basin, Kurdistan region, NE of Iraq using vulnerability mapping. Arab J. Geosci. 9, pp. 223. https://doi.org/10.1007/s12517-015-2264-y

Abdullah, T.O. Ali, S.S. Al-Ansari, N.A. Knutsson, S., 2019. Hydrogeochemical evaluation of groundwater and its suitability for domestic uses in Halabja Saidsadiq Basin, Iraq. Water, 11, pp. 690. https://doi.org/10.3390/w11040690

Aghazadeh, N., Chitsazan, M. and Golestan, Y., 2017. Hydrochemistry and quality assessment of groundwater in the Ardabil area, Iran. Applied Water Science, 7, pp.3599-3616. https://doi.org/10.1007/s13201-016-0498-9

Ahmed, A. and Clark, I., 2016. Groundwater flow and geochemical evolution in the Central Flinders Ranges, South Australia. Science of the Total Environment, 572, pp.837-851. https://doi.org/10.1016/j.scitotenv.2016.07.123

Al-Adili, A.S. and Ali, S.M., 2005. Hydrochemical Evolution of Shallow Ground Water System Within Baghdad City–Iraq. The Iraqi Geological Journal, pp.134-139.

Al-Ghanimy, M., Al-Mutawki, K.G. and Falah, H.H., 2019, September. Geochemical Modeling of Groundwater in AL Teeb Area (North East Missan Governorate). In Journal of Physics: Conference Series (Vol. 1294, No. 8, p. 082002). IOP Publishing.

Ali S. S., 2007.Geology and hydrogeology of Sharazoor-Piramagroon basin in Sulaimani area, northeastern Iraq. Unpublished PhD Thesis, University of Belgrade, Faculty of Mining and Geology, 330 P.

Al-Manmi, D.A., 2007. Groundwater quality evaluation in Kalar town-Sulaimani/NE-Iraq. Iraqi Journal of Earth Sciences, 7(2), pp.31-52.

Al-Manmi, D.A., Hamamin, D.F. and Salih, A.O., 2019. Karezes, abandoned and endangered water resources in semi-arid regions: case study from Sulaymaniyah City, Iraq. Iraqi Bulletin of Geology and Mining, 15(1), pp.91-104. https://www.iasj.net/iasj/download/c86b9b066d87390e

Al-Manmi, D.A.M., 2002. Chemical and environmental study of groundwater in Sulaymaniyah city and its outskirts. Unpublished master's thesis, University of Baghdad, College of Science, 200 pages. (In Arabic).

Al-Manmi, D.A.M.A. and Saleh, K.A., 2019. Delineation of spring protection zone and vulnerability mapping of selected springs in Sulaymaniyah area, Kurdistan, Iraq. Environmental Earth Sciences, 78, pp.1-16.

Al-Mansoori, H.B.G., 2000. Hydrogeochemical and the effect of pumping tests on the quality of groundwater in the Dibdiba aquifer, Safwan-Zubair, South of Iraq. Unpublished master's thesis, University of Basrah, College of Science, 143 pages. (In Arabic).

Al-Mashreki, M.H., Eid, M.H., Saeed, O., Székács, A., Szűcs, P., Gad, M., Abukhadra, M.R., AlHammadi, A.A., Alrakhami, M.S., Alshabibi, M.A. and Elsayed, S., 2023. Integration of Geochemical Modeling, Multivariate Analysis, and Irrigation Indices for Assessing Groundwater Quality in the Al-Jawf Basin, Yemen. Water, 15(8), pp.1496. https://doi.org/10.3390/w15081496

Al-Qurnawi, W.S., Ghalib, H.B., Alabadi, M.A. and Hawash, A.B.A., 2022. Corrosion-scaling potentially of domestic water pipelines and evaluate the applicability of raw water sources in Basrah, Iraq. Iraqi Journal of Science, pp.2089-2102.

Al-Shamari, M.M., 2017. Geochemical modeling of groundwater in the Dammam formation south of Razzaza lake, middle of Iraq. The Iraqi Geological Journal, pp.49-64.

Al-Tamimi, OS. 2007. "Water Resource Evaluation in Diyala River Basin, Middle part." Ph. D. thesis, College of Science, University of Baghdad, 235pp (in Arabic).

APHA, 2017. Standard Methods for the Examination of Water and Wastewater (23rd ed.). Washington DC American Public Health Association. https://yabesh.ir/wp-content/uploads/2018/02/Standard-Methods-23rd-Perv.pdf

Appelo, C.A.J. and Postma, D., 1999 Geochemistry. Groundwater and Pollution. Rotterdam, P.536.

Appelo, C.A.J. and Postma, D., 2004. Geochemistry, groundwater and pollution, 2nd edition. CRC press, 649 P.

Ball, J.W. and Nordstrom, D. K., 2003. WATEQ4F – A Computer Program for Calculating Speciation of Major, Trace and Redox Elements in Natural Water. USGS, Open file Report, pp. 91-189.

Ball, J.W. and Nordstrom, D.K., 1994. WATEQ4F – a computer program for calculating speciation of major, trace and redox elements in natural water. USGS, Open file Report, pp. 91-189.

Bellen, R.C., van Dunnington, H.V., Wezel, R. and Morton, D.M., 1959. Lexique stratigraphique international. Vol. III, Asie, Fasc. 10a, Iraq, Paris, 336 P.

Buday, T., 1980. The regional geology of Iraq, Vol I: Stratigraphy and Paleogeography. I.I.M. Kassab and S.Z. Jassim (eds). SOM, Baghdad, Dar El-Kutib Publ. House, Univ. of Mosul., 445 P.

Domenico, P.A. and Schwartz, F.W., 1998. Physical and Chemical Hydrogeology. John Wiley and Sons Inc., New York, 506 P.

Drever, J.I., 1997. The Geochemistry of Natural Water, Surface and Groundwater Environments, 3rd ed., Prentice Hall, USA, 436 P.

Eissa, M.A., 2018. Application of multi-isotopes and geochemical modeling for delineating recharge and salinization sources in Dahab basin aquifers (South Sinai, Egypt). Hydrology, 5(3), p.41. https://doi.org/10.3390/hydrology5030041

Eissa, M.A., Thomas, J.M., Hershey, R.L., Dawoud, M.I., Pohll, G., Dahab, K.A., Gomaa, M.A. and Shabana, A.R., 2014. Geochemical and isotopic evolution of groundwater in the Wadi Watir watershed, Sinai Peninsula, Egypt. Environmental earth sciences, 71, pp.1855-1869. https://doi.org/10.1007/s12665-013-2588-4

El Alfy, M., 2013. Hydrochemical modeling and assessment of groundwater contamination in Northwest Sinai, Egypt. Water environment research, 85(3), pp.211-223.https://doi.org/10.2175/106143012x13560205145055

El Alfy, M., Abdalla, F., Moubark, K. and Alharbi, T., 2019. Hydrochemical equilibrium and statistical approaches as effective tools for identifying groundwater evolution and pollution sources in arid areas. Geoscience journal, 23(2), pp.299-314. https://doi.org/10.1007/s12303-018-0039-7

El-Kadi, A.I., Plummer, L.N. and Aggarwal, P., 2011. NETPATH-WIN: An interactive user version of the mass-balance model, NETPATH. Groundwater, 49(4), pp.593-599. https://doi.org/10.1111/j.1745-6584.2010.00779.x

Gomaa, M.A., Emara, M.M., El-Sabbah, M.M.B. and Mohallel, S.A., 2014. Applications of Hydrogeochemical Modeling to Evaluate Quaternary Aquifer in the Area Between Idfu and Aswan, Eastern Desert, Egypt. International Journal of Water Resources and Arid Environments 3(1), p.19-34.

Hussein, H., Abd El-Raouf, A., Almadani, S., Abdelrahman, K., Ibrahim, E. and Osman, O.M., 2021. Application of geochemical modeling using NETPATH and water quality index for assessing the groundwater geochemistry in the south Wadi El-Farigh area, Egypt. Journal of King Saud University-Science, 33(2), pp.101284. https://doi.org/10.1016/j.jksus.2020.101284

Jassim, S. Z. and Goff, J. C., 2006. Geology of Iraq, 1st. Edited by Lea Novotna. Dolin, Hlavni 2732, Prague and Moravian Museum, Zelny trh 6, Brno, Czech Republic, 362 P.

Khosravi, R., Zarei, M. and Sracek, O., 2020. Hydraulic and geochemical interactions between surface water and sediment pore water in seasonal hypersaline Maharlu Lake, Iran. Hydrological Processes, 34, pp.3358–3369. https://doi.org/10.1002/hyp.13797

Kumar, A. Rout, S. Narayanan, U. Manish, K. Mishra, R. Tripathi, M. Singh, J. Kumar, S. Kushwaha, H.S., 2011.Geochemical modelling of uranium speciation in the subsurface aquatic environment of Punjab state in India. Journal of Geology and Mining Research, 3, pp.137–146.

Langmuir, D., 1997. Aqueous Environmental Geochemistry. Prentice Hall, USA, 600 P.

Mahmmud, R., Sracek, O., Mustafa, O., Čejková, B., Jačková, I. and Vondrovicová, L., 2022. Groundwater geochemistry evolution and geogenic contaminants in the Sulaimani-Warmawa Sub-basin, Sulaimani, Kurdistan Region, Iraq. Environmental Monitoring and Assessment, 194(5), pp.352. https://doi.org/10.1007/s10661-022-09933-6

Masoud, M., Rajmohan, N., Basahi, J., Schneider, M., Niyazi, B. and Alqarawy, A., 2022. Integrated Hydrogeochemical Groundwater Flow Path Modelling in an Arid Environment. Water, 14(23), pp.3823. https://doi.org/10.3390/w14233823

Melidis, P., Sanozidou, M., Mandusa, A. and Ouzounis, K., 2007. Corrosion control by using indirect methods. Desalination, 213(1-3), pp.152-158. https://doi.org/10.1016/j.desal.2006.03.606

Merkel, B.J., Planer-Friedrich, B. and Nordstrom, D.K., 2005. Groundwater geochemistry. A practical guide to modeling of natural and contaminated aquatic systems, 2.

Mustafa, O. Mahmmud, R. Sracek, O. Seeyan, S., 2023. Geogenic sources of Arsenic and Fluoride in groundwater: Examples from the Zagros Basin, the Kurdistan Region of Iraq. Water, 15, pp. 1981. https://doi.org/10.3390/w15111981

Parkhurst, D.L., and C.A.J. Appelo., 1999. User's guide to PHREEQC—a computer program for speciation, batchreaction, one-dimensional transport, and inverse geochemical calculations. Water-Resources Investigations Report 99- 4259. Reston, Virginia: U.S. Geological Survey, 312.

Parkhurst, D.L. and S.R. Charlton., 2008. NetpathXL—An Excel® Interface to the Program NETPATH. U.S. Geological Survey Techniques and Methods 6-A26, 11p. ftp://brrftp. cr.usgs.gov/geochem/pc/netpath/NetpathXL.pdf.

Plummer, L.N., 1992. Geochemical modeling of water rock interaction: past, present, future. In: Y. Khavaka and A. Maest (eds.): Proc. https://pascal-francis.inist.fr/vibad/index.php?action=getRecordDetail&idt=6462562

Plummer, L.N., L.M. Bexfield, S.K. Anderholm, W.E. Sanford and E. Busenberg, 2004. Geochemical characterization of ground-water flow in the Santa Fe Group aquifer system, Middle Rio Grande Basin, New Mexico. Water-Resources Investigations Report 03-4131. Reston, Virginia: U.S. Geological Survey, 395.http://pubs.usgs.gov/wri/wri034131/.

Plummer, L.N., Parkhurst, D.L. and Thorstenson, D.C., 1983. Development of reaction models for groundwater system. Geochemica et Cosmochemica Acta, 47, pp. 665-686.

Plummer, L.N., Prestemon, E.C. and Parkhurst, D.L.,1996. An interactive code (NETPATH) for modeling net geochemical reactions along a flowpath. USGS, Water Resources Investigations Report 91, 130p.

Polservice, 1980. Sharazoor irrigation project. Feasibility report, Annex I, Climate and Water resources, Ministry of Irrigation, Baghdad, 76p.

Stevanovic, Z. and Markovic, M. ,2004b. Hydrogeology of Northern Iraq.Vol.2, General Hydrogeology and Aquifer Systems. Food and Agriculture Organization of the United Nations, Rome.246 P.

Stuyfzand, P.J., 1999. Patterns in groundwater chemistry resulting from groundwater flow. Hydrogeology journal, 7, pp. 15-27. https://doi.org/10.1007/s100400050177

Varsanyi, I. and Kovacs, L.O., 1997. Chemical evolution of groundwater in the river Danube deposits in the southern part of the Pannonian Basin (Hungary). Appl. Geochem., 12, pp. 625-636. https://doi.org/10.1016/S0883-2927(97)00018-8

Wang, Y., T. Ma. and Z. Luo, 2001. Geostatistical and geochemical analysis of surface water leakage into groundwater on a regional scale: a case study in the Liulin Karst system, northwestern China Journal of Hydrology, 246, pp. 223-234. https://doi.org/10.1016/S0022-1694(01)00376-6

WHO., 2022. Guidelines for drinking-water quality: Fourth edition incorporating the first and second addenda (Fourth edition ed.). https://www.who.int/teams/environment-climate-change-and-health/water-sanitation-and-health/water-safety-and-quality/drinking-water-quality-guidelines

Wigley, T.M.L., L.N. Plummer and F.J. Pearson Jr., 1978. Mass transfer and carbon isotope evolution in natural water systems. Geochimica et Cosmochimica Acta 42, pp.1117–1139. https://doi.org/10.1016/0016-7037(78)90108-4

Wilkes University-Center of Environmental Quality, Geoenvironmental Sciences and Engineering Department W.U., C.E.G, G.S.E. Dept., 2002. "Corrosion, saturation index, balanced water in drinking water systems - Source and cause of corrosion". http://wilkes.edu/~eqc/corrosion.htm.

Yang, N., Wang, G., Shi, Z., Zhao, D., Jiang, W., Guo, L., Liao, F. and Zhou, P., 2018. Application of multiple approaches to investigate the hydrochemistry evolution of groundwater in an arid region: Nomhon, Northwestern China. Water, 10(11), pp.1667. https://doi.org/10.3390/w10111667

Appendix (1) Physical Parameters and Major Ions Concentrations in Water Wells Samples

Sample No.	TºC	pH	Eh (v)	EC	TDS	TH	unit	Ca^{2+}	Mg^{2+}	Na^{+}	K^{+}	SUM	$SO4^{2-}$	Cl^{-}	HCO_3^{-}	CO_3^{2-}	SUM
				µs/cm	mg/l												
W1	16.6	7.82	-56	730	467.2	334	ppm	95.10	23.50	13.60	1.80	134.00	72.00	14.00	260.00	0.00	346.00
							epm	4.76	1.96	0.59	0.05	7.35	1.50	0.39	4.26	0.00	6.15
							%epm	64.69	26.64	8.04	0.63	100.00	24.39	6.32	69.29	0.00	100.00
W2	13.1	7.80	-55	524	335.36	274	ppm	78.00	19.30	6.80	1.60	105.70	44.00	20.00	245.00	0.00	309.00
							epm	3.90	1.61	0.30	0.04	5.85	0.92	0.56	4.02	0.00	5.49
							%epm	66.72	27.52	5.06	0.70	100.00	16.70	10.12	73.18	0.00	100.00
W3	18.8	7.11	-23.8	715	457.6	312	ppm	91.20	20.40	12.70	1.90	126.20	78.00	16.00	258.00	0.00	352.00
							epm	4.56	1.70	0.55	0.05	6.86	1.63	0.44	4.23	0.00	6.30
							%epm	66.46	24.78	8.05	0.71	100.00	25.80	7.06	67.15	0.00	100.00
W4	14.2	7.30	-24	682	436.48	284	ppm	83.60	18.30	13.00	1.90	116.80	68.00	16.00	243.00	0.00	327.00
							epm	4.18	1.53	0.57	0.05	6.32	1.42	0.44	3.98	0.00	5.84
							%epm	66.15	24.13	8.94	0.77	100.00	24.24	7.60	68.16	0.00	100.00
W5	13.6	7.42	-33.2	684	437.76	300	ppm	84.00	22.00	8.00	2.70	116.70	70.00	15.00	246.00	0.00	331.00
							epm	4.20	1.83	0.35	0.07	6.45	1.46	0.42	4.03	0.00	5.91
							%epm	65.11	28.42	5.39	1.07	100.00	24.68	7.05	68.26	0.00	100.00

W6	15.1	7.26	-27	720	460.8	326	ppm	94.00	22.30	19.00	1.70	137.00	93.00	20.00	253.00	0.00	366.00
							epm	4.70	1.86	0.83	0.04	7.43	1.94	0.56	4.15	0.00	6.64
							%epm	63.27	25.02	11.12	0.59	100.00	29.18	8.37	62.46	0.00	100.00
W7	18	7.55	-44.4	395	252.8	203	ppm	62.00	11.60	9.00	1.80	84.40	25.00	19.00	198.00	0.00	242.00
							epm	3.10	0.97	0.39	0.05	4.50	0.52	0.53	3.25	0.00	4.29
							%epm	68.83	21.46	8.69	1.02	100.00	12.13	12.29	75.58	0.00	100.00
W8	19.3	8.4	-92.4	385	246.4	198	ppm	59.50	12.00	9.80	1.70	83.00	23.00	20.00	193.00	0.00	236.00
							epm	2.98	1.00	0.43	0.04	4.44	0.48	0.56	3.16	0.00	4.20
							%epm	66.93	22.50	9.59	0.98	100.00	11.41	13.23	75.36	0.00	100.00
W9	20	7.1	-26.7	277	177.28	154	ppm	45.00	10.00	8.00	1.50	64.50	18.00	20.00	182.00	0.00	220.00
							epm	2.25	0.83	0.35	0.04	3.47	0.38	0.56	2.98	0.00	3.91
							%epm	64.85	24.02	10.02	1.11	100.00	9.58	14.19	76.23	0.00	100.00
W10	20	7.5	-43	190	121.6	142	ppm	43.00	8.50	6.30	1.50	59.30	19.00	17.00	179.00	0.00	215.00
							epm	2.15	0.71	0.27	0.04	3.17	0.40	0.47	2.93	0.00	3.80
							%epm	67.81	22.34	8.64	1.21	100.00	10.41	12.42	77.17	0.00	100.00
W11	20.6	7.2	-29.5	266	170.24	156	ppm	47.00	9.50	8.20	1.40	66.10	18.30	22.00	181.00	0.00	221.30
							epm	2.35	0.79	0.36	0.04	3.53	0.38	0.61	2.97	0.00	3.96
							%epm	66.50	22.40	10.09	1.02	100.00	9.63	15.43	74.94	0.00	100.00
W12	19.5	7.1	-20	350	224	172	ppm	52.00	10.20	11.20	0.10	73.50	26.00	18.00	190.00	0.00	234.00
							epm	2.60	0.85	0.49	0.00	3.94	0.54	0.50	3.11	0.00	4.16
							%epm	66.00	21.58	12.36	0.07	100.00	13.03	12.03	74.94	0.00	100.00
W13	19.5	7		255	163.2	152	ppm	45.70	9.10	6.50	0.10	61.40	17.60	19.00	182.00	0.00	218.60

			-17				epm	2.29	0.76	0.28	0.00	3.33	0.37	0.53	2.98	0.00	3.88
							%epm	68.65	22.78	8.49	0.08	100.00	9.45	13.61	76.94	0.00	100.00
W14	19.7	7.3	-30.6	215	137.6	132	ppm	41.00	7.30	5.60	0.10	54.00	6.70	9.00	186.00	0.00	201.70
							epm	2.05	0.61	0.24	0.00	2.90	0.14	0.25	3.05	0.00	3.44
							%epm	70.58	20.95	8.38	0.09	100.00	4.06	7.27	88.67	0.00	100.00
W15	20.6	6.92	-12.7	452	289.28	237	ppm	70.00	15.20	13.80	0.60	99.60	48.00	14.00	214.00	0.00	276.00
							epm	3.50	1.27	0.60	0.02	5.38	1.00	0.39	3.51	0.00	4.90
							%epm	65.03	23.54	11.15	0.29	100.00	20.42	7.94	71.64	0.00	100.00
W16	21.5	7.7	-46.3	204	130.56	138	ppm	44.00	6.80	6.70	0.10	57.60	26.00	7.00	176.00	0.00	209.00
							epm	2.20	0.57	0.29	0.00	3.06	0.54	0.19	2.89	0.00	3.62
							%epm	71.88	18.52	9.52	0.08	100.00	14.96	5.37	79.67	0.00	100.00
W17	20.4	7	-17.2	308	197.12	160	ppm	48.00	9.70	8.90	0.00	66.60	37.50	12.00	188.00	0.00	237.50
							epm	2.40	0.81	0.39	0.00	3.60	0.78	0.33	3.08	0.00	4.20
							%epm	66.75	22.48	10.76	0.00	100.00	18.62	7.94	73.44	0.00	100.00
W18	18.5	7.2	-28.2	274	175.36	174	ppm	50.00	12.00	9.20	0.00	71.20	52.00	9.00	190.00	0.00	251.00
							epm	2.50	1.00	0.40	0.00	3.90	1.08	0.25	3.11	0.00	4.45
							%epm	64.10	25.64	10.26	0.00	100.00	24.36	5.62	70.02	0.00	100.00
W19	19	7.1	-26	236	151.04	147	ppm	45.00	8.30	9.50	0.10	62.90	32.00	11.00	178.00	0.00	221.00
							epm	2.25	0.69	0.41	0.00	3.36	0.67	0.31	2.92	0.00	3.89
							%epm	67.02	20.60	12.30	0.08	100.00	17.14	7.85	75.01	0.00	100.00
W20	20.7	7	-14.4	454	290.56	249	ppm	72.00	16.80	11.30	2.70	102.80	54.00	14.00	219.00	0.00	287.00
							epm	3.60	1.40	0.49	0.07	5.56	1.13	0.39	3.59	0.00	5.10

							%epm	64.74	25.18	8.84	1.25	100.00	22.04	7.62	70.34	0.00	100.00
W21	18.8	7.1	-24	306	195.84	154	ppm	46.00	9.50	10.50	0.30	66.30	21.00	13.00	189.00	0.00	223.00
							epm	2.30	0.79	0.46	0.01	3.56	0.44	0.36	3.10	0.00	3.90
							%epm	64.68	22.26	12.84	0.22	100.00	11.23	9.27	79.51	0.00	100.00
W22	18.8	7.5	-49.4	526	336.64	271	ppm	75.00	20.30	7.00	0.10	102.40	28.00	16.00	258.00	0.00	302.00
							epm	3.75	1.69	0.30	0.00	5.75	0.58	0.44	4.23	0.00	5.26
							%epm	65.23	29.43	5.29	0.04	100.00	11.10	8.45	80.45	0.00	100.00
W23	19.1	7.6	-45.4	336	215.04	190	ppm	53.00	13.90	11.80	0.10	78.80	36.00	14.00	196.00	0.00	246.00
							epm	2.65	1.16	0.51	0.00	4.32	0.75	0.39	3.21	0.00	4.35
							%epm	61.29	26.79	11.87	0.06	100.00	17.23	8.94	73.83	0.00	100.00
W24	18.8	7.21	-27.5	422	270.08	228	ppm	69.00	13.50	10.80	0.50	93.80	43.00	15.00	200.00	0.00	258.00
							epm	3.45	1.13	0.47	0.01	5.06	0.90	0.42	3.28	0.00	4.59
							%epm	68.22	22.24	9.28	0.25	100.00	19.51	9.08	71.41	0.00	100.00
W25	18.7	7	-22	382	244.48	188	ppm	57.00	11.00	8.70	0.60	77.30	22.00	17.00	190.00	0.00	229.00
							epm	2.85	0.92	0.38	0.02	4.16	0.46	0.47	3.11	0.00	4.05
							%epm	68.50	22.03	9.09	0.37	100.00	11.33	11.67	77.00	0.00	100.00
W26	17.6	6.97	-14.4	332	212.48	177	ppm	51.40	11.80	8.30	0.10	71.60	40.00	10.00	192.00	0.00	242.00
							epm	2.57	0.98	0.36	0.00	3.92	0.83	0.28	3.15	0.00	4.26
							%epm	65.62	25.11	9.21	0.07	100.00	19.57	6.52	73.91	0.00	100.00
W27	20	7.38	-42	343	219.52	192	ppm	53.00	14.60	12.00	0.20	79.80	36.00	10.00	195.00	0.00	241.00 0
							epm	2.65	1.22	0.52	0.01	4.39	0.75	0.28	3.20	0.00	4.22
							%epm	60.32	27.69	11.88	0.12	100.00	17.75	6.58	75.67	0.00	100.00

W28	18.8	7.5	-41.5	465	297.6	261	ppm	75.00	18.00	13.00	0.10	106.10	56.00	13.00	223.00	0.00	292.00
							epm	3.75	1.50	0.57	0.00	5.82	1.17	0.36	3.66	0.00	5.18
							%epm	64.46	25.78	9.72	0.04	100.00	22.51	6.97	70.53	0.00	100.00
W29	19.3	7.2	-26	270	172.8	162	ppm	48.00	10.20	8.90	0.10	67.20	23.00	13.00	183.00	0.00	219.00
							epm	2.40	0.85	0.39	0.00	3.64	0.48	0.36	3.00	0.00	3.84
							%epm	65.94	23.35	10.63	0.07	100.00	12.48	9.40	78.12	0.00	100.00
W30	18.7	7.33	-31	198	126.72	137	ppm	43.00	7.20	10.00	0.20	60.40	22.00	12.00	170.00	0.00	204.00
							epm	2.15	0.60	0.43	0.01	3.19	0.46	0.33	2.79	0.00	3.58
							%epm	67.40	18.81	13.63	0.16	100.00	12.81	9.31	77.88	0.00	100.00
W31	20	7.25	-27.2	362	231.68	202	ppm	54.00	16.30	13.00	0.20	83.50	39.00	11.00	199.00	0.00	249.00
							epm	2.70	1.36	0.57	0.01	4.63	0.81	0.31	3.26	0.00	4.38
							%epm	58.33	29.35	12.21	0.11	100.00	18.55	6.98	74.48	0.00	100.00
W32	17.2	7.72	-43	470	300.8	272	ppm	76.00	20.00	16.00	0.00	112.00	58.00	15.00	225.00	0.00	298.00
							epm	3.80	1.67	0.70	0.00	6.16	1.21	0.42	3.69	0.00	5.31
							%epm	61.67	27.05	11.29	0.00	100.00	22.74	7.84	69.42	0.00	100.00
W33	18.8	8.1	-68.7	750	480	268	ppm	103.00	27.00	33.00	0.60	163.60	86.00	44.00	268.00	0.00	398.00
							epm	5.15	2.25	1.43	0.02	8.85	1.79	1.22	4.39	0.00	7.41
							%epm	58.19	25.42	16.21	0.17	100.00	24.19	16.50	59.31	0.00	100.00
Min.	13.10	6.92	-92.4	190.00	121.6	132	ppm	41.00	6.80	5.60	0.00		6.70	7.00	170.00	0.00	
							epm	2.05	0.57	0.24	0.00		0.14	0.19	2.79	0.00	
							%epm	58.19	18.52	5.06	0.00		4.06	5.37	59.31	0.00	
Max.	21.50	8.40		750.00	480	480	ppm	103.00	27.00	33.00	2.70		93.00	44.00	268.00	0.00	

			-12.7				epm	5.15	2.25	1.43	0.07		1.94	1.22	4.39	0.00	
							%epm	71.88	29.43	16.21	1.25		29.18	16.50	88.67	0.00	
Mean	18.58	7.35	-34.23	408.42	261.39	213.50	ppm	62.23	14.12	10.91	0.80		40.55	15.61	207.55	0.00	
							epm	3.11	1.18	0.47	0.02		0.84	0.43	3.40	0.00	
							%epm	65.51	24.12	9.97	0.41		17.07	9.30	73.63	0.00	

Appendix (2) Physical Parameters and Major Ions Concentrations in Springs Water Samples

Sample No.	ToC	pH	Eh (v)	EC	TDS	TH	unit	Ca2+	Mg2+	Na+	K+	SUM	SO42-	Cl-	HCO3-	CO32-	SUM
				µs/cm	mg/l												
S1	17.80	7.34	-29.4	391	250.24	209	ppm	59.00	15.00	9.30	0.40	83.70	42.00	16.00	213.00	0.00	271.00
							epm	2.95	1.25	0.40	0.01	4.61	0.88	0.44	3.49	0.00	4.81
							%epm	63.93	27.09	8.76	0.22	100.00	18.19	9.24	72.58	0.00	100.00
S2	13.50	8.54	-95	294	188.16	191	ppm	50.00	16.00	6.90	0.10	73.00	25.00	6.00	200.00	0.00	231.00
							epm	2.50	1.33	0.30	0.00	4.14	0.52	0.17	3.28	0.00	3.97
							%epm	60.45	32.24	7.25	0.06	100.00	13.13	4.20	82.67	0.00	100.00
S3	29.00	6.5	8.8	1890	1209.6	928	ppm	215.00	95.00	52.00	8.40	370.40	486.00	33.00	375.00	0.00	894.00
							epm	10.75	7.92	2.26	0.22	21.14	10.13	0.92	6.15	0.00	17.19
							%epm	50.84	37.44	10.69	1.02	100.00	58.90	5.33	35.76	0.00	100.00
S4	14.80	7.25	-27.1	448	286.72	248	ppm	73.00	16.00	8.50	0.20	97.70	46.00	17.00	218.00	0.00	281.00
							epm	3.65	1.33	0.37	0.01	5.36	0.96	0.47	3.57	0.00	5.00
							%epm	68.12	24.88	6.90	0.10	100.00	19.15	9.44	71.41	0.00	100.00
S5	15.10	7.24	-22.2	460	294.4	233	ppm	72.00	13.00	8.10	0.30	93.40	22.00	7.00	216.00	0.00	245.00
							epm	3.60	1.08	0.35	0.01	5.04	0.46	0.19	3.54	0.00	4.19
							%epm	71.38	21.48	6.98	0.15	100.00	10.93	4.64	84.43	0.00	100.00
S6	13.40	7.53	-32.2	432	276.48	203	ppm	65.00	10.00	8.50	0.50	84.00	28.00	11.00	198.00	0.00	237.00

							epm	2.00	0.98	0.42	0.01	3.41	0.44	0.25	2.92	0.00	3.61
							%epm	58.70	28.62	12.38	0.30	100.00	12.13	6.93	80.93	0.00	100.00
Min.	13.40	6.50	-95	226.00	144.64	148	ppm	40.00	10.00	6.90	0.10		21.00	6.00	178.00	0.00	
							epm	2.00	0.83	0.30	0.00		0.44	0.17	2.92	0.00	
							%epm	50.84	18.66	6.90	0.06		10.93	4.20	35.76	0.00	
Max.	29.00	8.54	8.8	1890.00	1209.60	928	ppm	215.00	95.00	52.00	8.40		486.00	33.00	375.00	0.00	
							epm	10.75	7.92	2.26	0.22		10.13	0.92	6.15	0.00	
							%epm	72.78	37.44	12.38	1.02		58.90	9.44	84.43	0.00	
Mean	17.34	7.34	-31.01	591.57	378.61	308.63	ppm	82.00	25.24	14.71	1.47		95.71	14.14	228.29	0.00	
							epm	4.10	2.10	0.64	0.04		1.99	0.39	3.74	0.00	
							%epm	63.74	27.20	8.75	0.31		20.93	6.74	72.33	0.00	